PRAMANA — journal of physics

Vol. 85, No. 1
July 2015
pp. 77–89

Bose–Einstein condensation in generalized Pöschl–Teller potential

SARATH R[1,*] and P C VINODKUMAR[2]

[1]Department of Applied Physics, Indian School of Mines, Dhanbad 826 004, India
[2]Department of Physics, Sardar Patel University, Vallabh Vidyanagar 388 120, India
*Corresponding author. E-mail: sarath91@live.com

MS received 24 August 2013; revised 20 June 2014; accepted 15 July 2014
DOI: 10.1007/s12043-014-0890-7; ***e*Publication:** 13 December 2014

Abstract. We analyse and explore some peculiar features of the generalized Pöschl–Teller potential. This particular potential can be tuned in terms of the allowed number of excited states, the shape of the potential, and the strength of the confinement. As an application we investigate the Bose–Einstein condensation of noninteracting ^{39}K atoms in this trapping potential. We numerically study the effect of different tuning schemes of this particular potential on the dynamics of noninteracting BEC.

Keywords. Trapping potential; Bose–Einstein condensation; supersymmetric quantum mechanics.

PACS No. 05.30.Jp

1. Introduction

Potentials have a wide range of applications, especially in the physics of cold trapped atoms, which is one of the frontier areas of modern research. Bose–Einstein condensation [1–6] is an important quantum mechanical phenomenon, as it elevates the quantum behaviour to macroscopic scale. Coherent matter waves and superfluidity are fascinating phenomena which arise from Bose–Einstein condensation [7]. Trapping potential plays an incredible role in the Bose–Einstein condensation. The phase space density can be increased by modifying the shape of the trapping potential [8]. The present study investigates the Bose–Einstein condensation in the generalized Pöschl–Teller potential.

The generalized Pöschl–Teller potential is not an exactly solvable potential in the ordinary quantum mechanics. However, in the supersymmetric quantum mechanics (SUSY QM) it is exactly solvable [9]. A detailed analysis of this particular potential is not available in literature. This may be due to the complex mathematical form of this radial potential. The solutions obtained in the SUSY QM and the similarity with the Morse potential, help us to analyse this particular potential. A very recent work on Morse potential [10] shows that the Morse potential can be tuned from a strong confining potential to a

free particle one. We aim to modify the generalized Pöschl–Teller potential in a similar way, so that we can study the dynamics of the noninteracting BEC with the evolution of the potential.

Two-body interaction is very important in the context of Bose–Einstein condensation [11,12]. The most attractive candidates like ^{23}Na and ^{87}Rb, which favour the preparation process through their collision properties, have strong repulsive interaction [4,5,12]. However, in the current scenario, an ideal Bose–Einstein condensate is very important. It is not only just because switching off the interatomic interaction makes the system simpler, but also because of its practical applications. The use of ideal Bose–Einstein condensate for the study of Anderson localization explores new interests in physics [12–14]. Introduction of even a weak interaction to the systems for such studies can hide the underlying physics of interest [12]. An ideal BEC would be an excellent candidate for the study of matter–wave interferometry, one of the promising field in modern physics [12,15–17]. An atomic gas of ^{39}K is a good choice for such studies of ideal BEC. In the present article, we discuss the Bose–Einstein condensation of noninteracting ^{39}K atoms in the generalized Pöschl–Teller potential.

The paper is organized in four parts. In the second part we analyse the generalized Pöschl–Teller potential and different possible tunings. In the third part we employ this potential and its features for the study of noninteracting BEC. In the fourth and the last section we draw important conclusions of the present study.

2. Generalized Pöschl–Teller potential

In SUSY QM, we shift the potential to make the ground-state energy zero, without any loss of generality. We begin our discussion by considering the shifted generalized Pöschl–Teller potential [9], which is a central potential, given as

$$V(r) = A^2 + (A^2 + B^2 + A\alpha)\mathrm{csch}^2(\alpha r) - B(2A + \alpha)\coth(\alpha r)\mathrm{csch}(\alpha r) \quad (1)$$

where $A < B$ and $A, B, \alpha > 0$. By SUSY QM its energy eigenvalue is given [9] as

$$E_n = A^2 - (A - n\alpha)^2 \quad (2)$$

with the quantum number, $n = 0, 1, 2, \ldots$ Here the potential and energy eigenvalue are given in the units $\hbar = 2m = 1$.

First-order energy difference, i.e. the energy difference between two consecutive energy levels E_n and $E_{(n+1)}$, is obtained as

$$\Delta'_n = 2A\alpha - \alpha^2(2n + 1). \quad (3)$$

The second-order energy difference is defined as the difference between two consecutive first-order differences, and is obtained as

$$\Delta''_n = -2\alpha^2 < 0. \quad (4)$$

So, eq. (3) restricts the number of physically allowed excited states as Δ'_n cannot be negative. Thus, the choice of A/α restricts the maximum value of n for excited states of the system and is given by

$$n_{\max} = \frac{A}{\alpha} - \frac{1}{2} \geq 0. \quad (5)$$

For all the choices of $n > n_{\max}$, the first-order energy difference will be negative and it represents an unphysical situation where $E_{n+1} < E_n$. As n starts with zero, $n_{\max}$ is the number of excited states, n_{exc}. As n_{exc} represents an integer and to make sure that eq. (5) results in an integer value, we rewrite eq. (5) as

$$n_{\text{exc}} = \frac{A}{\alpha} - 1 \tag{6}$$

such that, even if A/α is a fraction, we shall approximate it to the very next integer, irrespective of the fractional part. This approximation is validated by looking into the nodes of the wave function given by [9],

$$\begin{aligned}\psi_n \;=\; & N_n(\cosh(\alpha r) - 1)^{((B-A)/2\alpha)}(\cosh(\alpha r) + 1)^{((-B-A)/2\alpha)} \\ & \times P_n^{((B/\alpha)-(A/\alpha)-(1/2),(-(B/\alpha)-(A/\alpha)-(1/2)))}(\cosh(\alpha r))\end{aligned} \tag{7}$$

for each n. The special function in eq. (7) is the Jacobi polynomial and N_n is the normalization constant. Equation (6) practically is a very important relation, as we can set the number of allowed energy excited states for the system by tuning the parameters A and α. So, unlike other potentials used for BEC, here we can tune the number of allowed energy states.

For a chosen physical system, we consider the time-independent Schrödinger equation,

$$-\frac{\hbar^2}{2m}\nabla^2\psi + V(r)\psi = E\psi, \tag{8}$$

where $V(r) = V'(r) + V_0$. $V(r)$ is the shifted generalized Pöschl–Teller potential (eq. (1) represents it in the dimension $\hbar = 2m = 1$), $V'(r)$ is the actual generalized Pöschl–Teller potential and V_0 is a constant so that the ground-state energy will be shifted appropriately to zero. Equation (8) can be reduced to

$$-\nabla^2\psi + \frac{2m}{\hbar^2}V(r)\psi = \frac{2m}{\hbar^2}E\psi. \tag{9}$$

Here $(2m/\hbar^2)V(r)$ is given by eq. (1). Hence, the shifted generalized Pöschl–Teller potential in the dimension of energy is given as

$$\begin{aligned}V(r) \;=\; & \frac{\hbar^2}{2m}(A^2 + (A^2 + B^2 + A\alpha)\text{csch}^2(\alpha r) \\ & -B(2A + \alpha)\coth(\alpha r)\text{csch}(\alpha r)).\end{aligned} \tag{10}$$

From eq. (10) we obtain the actual generalized Pöschl–Teller potential $V'(r)$ and the constant V_0 as

$$\begin{aligned}V'(r) = & \frac{\hbar^2}{2m}((A^2 + B^2 + A\alpha)\text{csch}^2(\alpha r) \\ & -B(2A + \alpha)\coth(\alpha r)\text{csch}(\alpha r))\end{aligned} \tag{11}$$

$$V_0 = \frac{\hbar^2}{2m}A^2. \tag{12}$$

$(2m/\hbar^2)E$ is given by eq. (2). Hence, the energy eigenvalue for the shifted generalized Pöschl–Teller potential, in the dimension of energy is

$$E_n = \frac{\hbar^2}{2m}(A^2 - (A - n\alpha)^2). \tag{13}$$

The energy eigenvalue for the actual system is given by

$$E'_n = E_n - V_0. \tag{14}$$

This can be obtained as

$$E'_n = -\frac{\hbar^2}{2m}(A - n\alpha)^2. \tag{15}$$

By the relation given in eq. (6), the energy eigenvalue for the actual system can be expressed as

$$E'_n = -\frac{\hbar^2}{2m}\alpha^2(n_{\text{exc}} - n + 1)^2, \tag{16}$$

where n_{exc} is the number of excited states and n is the quantum number as mentioned above.

It can easily be seen that for the choices of the parameters B, the shape of the potential can be tuned. For this we take B as

$$B = A + \beta\alpha, \tag{17}$$

where β is a dimensionless number. By tuning β we can tune the shape of the potential. For $0 < \beta < 1$, i.e., $A < B < (A + \alpha)$, the shape of the generalized Pöschl–Teller potential in three dimensions looks like a funnel. For $\beta > 1$, i.e., $B > (A + \alpha)$, the shape of the potential is so much similar to the shape of the Morse potential.

By the relations (6) and (17), the shifted generalized Pöschl–Teller potential given in eq. (10) can be represented as

$$\begin{aligned} V(r) = \frac{\hbar^2}{2m}(&\alpha^2((1 + n_{\text{exc}})^2 - (3 + 2n_{\text{exc}})(1 + n_{\text{exc}} + \beta)\coth(r\alpha)\text{csch}(r\alpha) \\ &+(3 + 5n_{\text{exc}} + 2n_{\text{exc}}^2 + 2(1 + n_{\text{exc}})\beta + \beta^2)\text{csch}^2(r\alpha))) \end{aligned} \tag{18}$$

For $\beta = 1$, the potential given in eq. (12) will reduce to

$$V(r) = \frac{\hbar^2}{2m}\left(\frac{1}{2}\alpha^2\left(2(1 + n_{\text{exc}})^2 - (2 + n_{\text{exc}})(3 + 2n_{\text{exc}})\text{sech}^2\left(\frac{\alpha r}{2}\right)\right)\right). \tag{19}$$

Dimensional analyses of eq. (1) show that A, B and α have the dimension of $[\text{Length}]^{-1}$. A very recent study of BEC in Morse potential [10] defines the argument part, i.e., the inverse confining length of the Morse potential as

$$\alpha = \sqrt{\frac{8mD}{\eta^2\hbar^2}}. \tag{20}$$

Considering the significant similarity of the generalized Pöschl– Teller potential to the Morse potential, we take α, the inverse confining length of the generalized Pöschl–Teller

potential in the same form as given in eq. (20), where D is the depth of the potential and η is a dimensionless number. By tuning η we can tune the potential from a strong confining potential to a free particle one as in ref. [10].

As harmonic potential is the simplest and the most favourable potential for the BEC, we equate the energy level difference between the first excited state and the ground state of generalized Pöschl–Teller potential to that of the harmonic potential, in order to get a physically meaningful value for the depth, D. For that, we assume that the frequency of the trap is the same in all directions and we take it as $\omega = 2\pi \times 65$ [12]. The energy difference between two consecutive energy levels (n and $n+1$) is $(\hbar^2/2m)\Delta'_n$. Hence equating the energy difference between the first excited state and the ground state of the generalized Pöschl–Teller potential with $\hbar\omega$, for 10^4 number of ^{39}K atoms, by setting $\eta = 1$, we obtain the depth $D = 5.38341 \times 10^{-37}$ J, where mass of a ^{39}K atom is $m = 6.4700806796142 \times 10^{-26}$ kg. We shall keep this value for D constant, throughout the present study. The shifted generalized Pöschl–Teller potential corresponding to n_{exc} tuning, β tuning and η tuning are shown in figures 1, 2 and 3 respectively. The shifted potentials are given in the dimension $\hbar = 2m = 1$.

Figures 1 and 3 show two different ways to tune the generalized Pöschl–Teller potential from a strong confining potential to a free particle one. Figure 2 shows that by choosing suitable value for β we can adjust the shape of the confining potential. However, as the energy eigenvalue of the generalized Pöschl–Teller potential does not depend on β or B, the dynamics of the noninteracting BEC will not be affected by β tuning.

3. BEC in a three-dimensional generalized Pöschl–Teller potential

Here we consider the Bose–Einstein condensation of N noninteracting atoms of ^{39}K trapped in a 3D generalized Pöschl–Teller potential. We aim to study the effects of different tuning schemes as mentioned in the previous section. For the ease of calculation, we consider the shifted generalized Pöschl–Teller potential. Similar analyses are

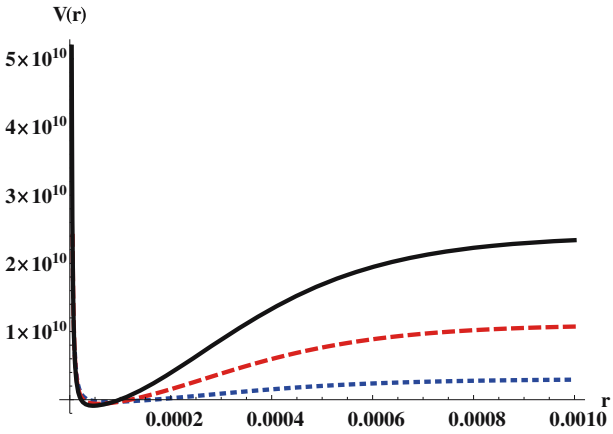

Figure 1. Variation of shifted potential $V(r)$ with respect to the tuning in the number of excited states, n_{exc}, for $\beta = 1.5$ and $\eta = 1$. The dotted blue line is for $n_{\text{exc}} = 10$, the red dashed line is for $n_{\text{exc}} = 20$ and the solid black line is for $n_{\text{exc}} = 30$.

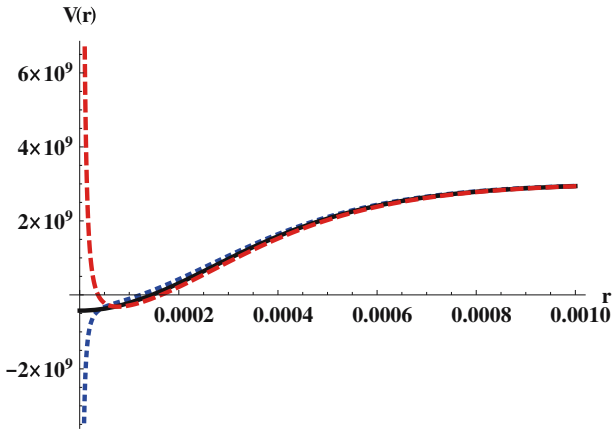

Figure 2. Variation of shifted potential $V(r)$ with respect to the tuning of β, for $n_{\text{exc}} = 10$ and $\eta = 1$. The dotted blue line is for $\beta = 0.5$, the solid black line is for $\beta = 1$ and the red dashed line is for $\beta = 1.5$.

available in [18]. However, in the present case, it has been possible to tune the potential in three different ways as we described in the previous section.

We investigate the effect of different tuning schemes of the potential on transition temperature (T_c). For this, we consider the condensation of $N = 10^4$ atoms. We take the mass of ^{39}K atom in kilogram as mentioned in the previous section, so that the energy will be in Joule. Now by equating the chemical potential to the ground-state energy ($\mu = E_0$), critical temperature (T_c) can be obtained from the relation given by [18]

$$N \approx \sum_{n=1}^{n_{\max}} \frac{1}{e^{(\beta_c E_n)} - 1}, \tag{21}$$

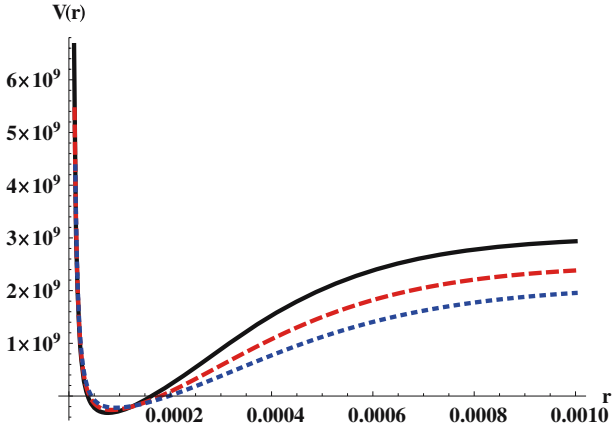

Figure 3. Variation of shifted potential $V(r)$ with respect to the tuning of η, for $n_{\text{exc}} = 10$ and $\beta = 1.5$. The solid black line is for $\eta = 1$, the red dashed line is for $\eta = 1.1$ and the dotted blue line is for $\eta = 1.2$.

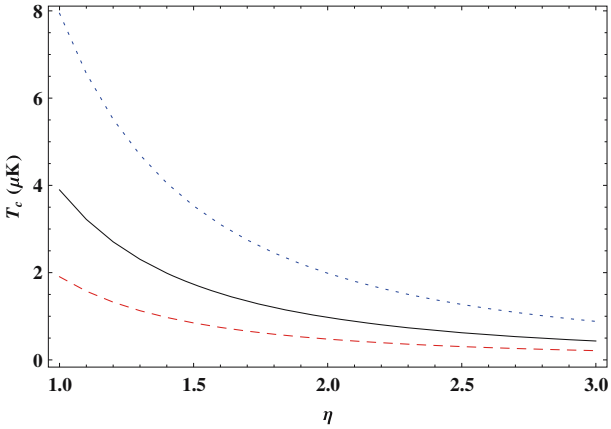

Figure 4. Variation in transition temperature (T_c) with respect to the η tuning, for different values of n_{exc}. The red dashed line is for $n_{exc} = 5000$, the solid black line is for $n_{exc} = 10^4$ and the blue dotted line is for $n_{exc} = 20000$. Here $N = 10^4$.

where $\beta_c = 1/(k_B T_c)$ at $T = T_c$ and E_n is the energy eigenvalue of the nth state. Equation (21) is solved numerically to get the value of T_c. The variation of T_c for η tuning corresponding to different choices of the excited states n_{exc} and the number of particles N are shown in figures 4 and 5 respectively.

Increase in n_{exc} and decrease in η increase the strength of the confinement. As the strength of the confinement decreases, the particle becomes more free, hence further lowering in T_c is needed for the condensation to take place. Figure 5 shows the effect of the number of ^{39}K atoms trapped in the potential. As the number of particles increases by keeping the strength of the potential constant, the transition temperature also increases.

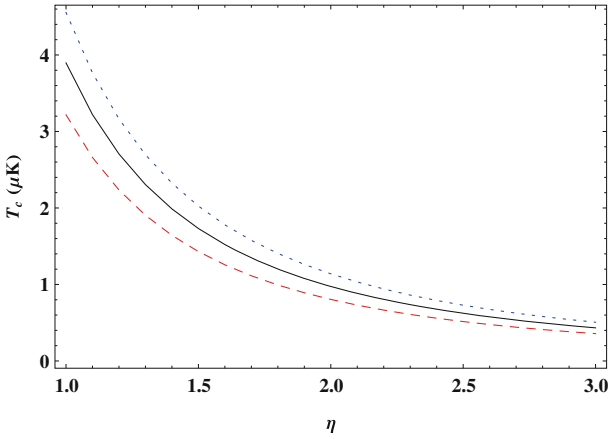

Figure 5. Variation in transition temperature (T_c) with respect to the η tuning, for different values of N. The red dashed line is for $N = 8000$, the solid black line is for $N = 10^4$ and the blue dotted line is for $N = 12000$. Here $n_{exc} = 10^4$.

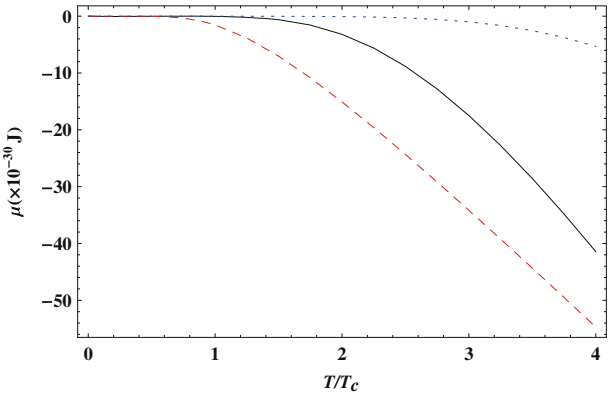

Figure 6. Chemical potential μ vs. T/T_c for different values of n_{exc}. The red dashed line is for $n_{exc} = 5000$, the solid black line is for $n_{exc} = 10^4$ and the blue dotted line is for $n_{exc} = 20000$. Here $\eta = 1$ and $N = 10^4$.

Now the chemical potential (μ) can be obtained, for a gas of N identical bosons, by solving the relation

$$N = \sum_{n=0}^{n_{max}} \frac{1}{e^{\beta_c(E_n-\mu)} - 1} \tag{22}$$

which can be rewritten as

$$N = N_0 + \sum_{n=1}^{n_{max}} \frac{1}{e^{\beta_c(E_n-\mu)} - 1}, \tag{23}$$

where

$$N_0 = \frac{1}{e^{\beta_c(E_0-\mu)} - 1}, \tag{24}$$

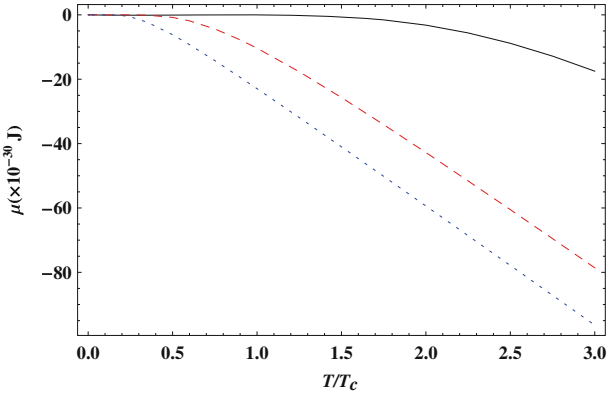

Figure 7. Chemical potential μ vs. T/T_c for different values of η. The solid black line is for $\eta = 1$, the red dashed line is for $\eta = 2$ and the dotted blue line is for $\eta = 3$. Here $n_{exc} = 10^4$ and $N = 10^4$.

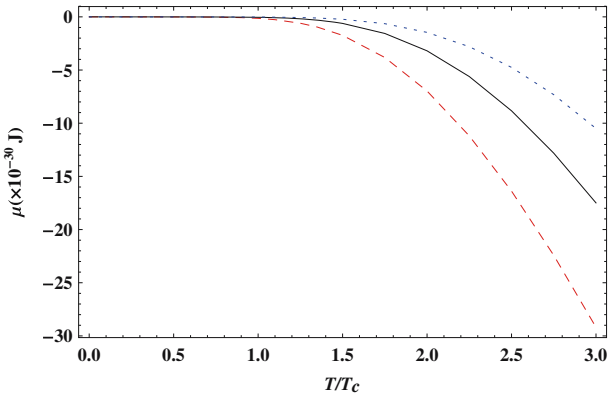

Figure 8. Chemical potential μ vs. T/T_c for different values of N. The red dashed line is for $N = 8000$, the solid black line is for $N = 10^4$ and the blue dotted line is for $N = 12000$. Here $\eta = 1$ and $n_{exc} = 10^4$.

where E_n is the energy of the nth state. The variation of μ as a function of T/T_c for the allowed different choices of number of excited states n_{exc}, parameter η and number of particles N are shown in figures 6, 7 and 8 respectively. Figures 6 and 7 show that, as the strength of the confinement increases by increasing the number of excited states n_{exc} and decreasing η at a particular temperature, the chemical potential increases. Chemical potential is defined as the change in energy of the system when a particle is removed from the system. As the confinement increases by increasing n_{exc} and decreasing η, the magnitude of the energy eigenvalue of the excited state increases. This is why the chemical potential increases as n_{exc} increases and η decreases for a particular temperature. Figure 8 shows that increase in N at a particular temperature increases the

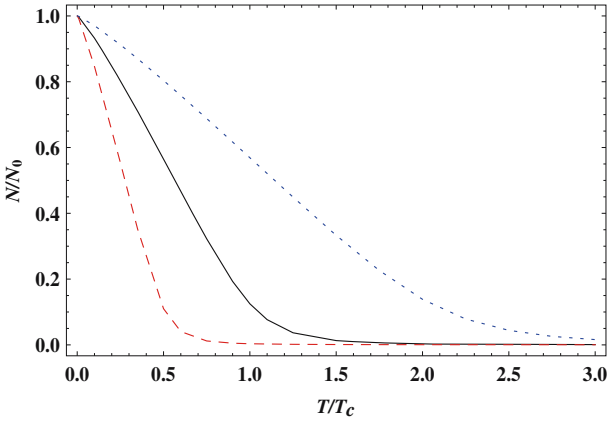

Figure 9. Condensate fraction vs. T/T_c for different values of n_{exc}. The red dashed line is for $n_{exc} = 5000$, the solid black line is for $n_{exc} = 10^4$ and the blue dotted line is for $n_{exc} = 20000$. Here $N = 10^4$ and $\eta = 1$.

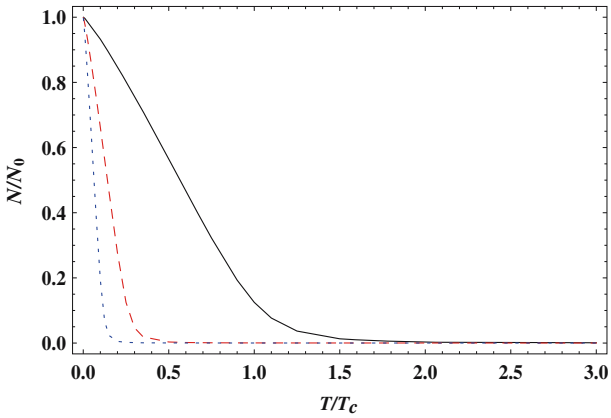

Figure 10. Condensate fraction vs. T/T_c for different values of η. The black solid line is for $\eta = 1$, the red dashed line is for $\eta = 2$ and the blue dotted line is for $\eta = 3$. Here $N = 10^4$ and $n_{exc} = 10^4$.

chemical potential. This can be understood from the definition of the chemical potential itself.

The average number of particles in the ground state can be obtained by substituting μ in eq. (24). For $N = 10^4$, $\eta = 1$ and for $n_{exc} = 5000, 10^4, 20000$, the condensate fraction as a function of T/T_c are computed and the results are shown in figure 9. Figure 10 shows the condensate fraction as a function of temperature for $n_{exc} = 10^4$, $N = 10^4$ and for $\eta = 1, 2, 3$. Figure 11 shows similar results for the condensate fraction as a function of temperature for $n_{exc} = 10^4$, $\eta = 1$ and for $N = 8000, 10^4, 12000$. It is clear that as the strength of the confinement and particle decreases for a particular temperature, the condensate fraction decreases.

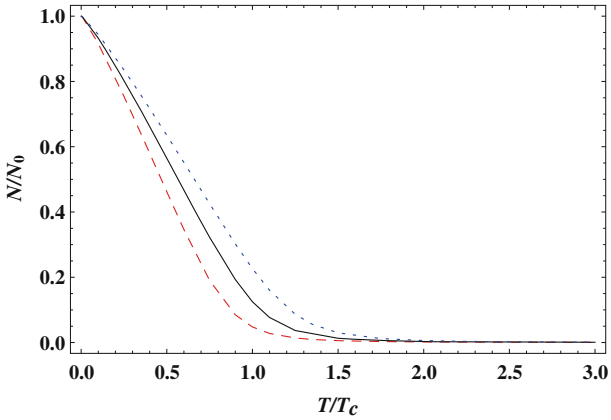

Figure 11. Condensate fraction vs. T/T_c for different values of N. The red dashed line is for $N = 8000$, the black solid line is for $N = 10^4$ and the blue dotted line is for $N = 12000$. Here $\eta = 1$ and $n_{exc} = 10^4$.

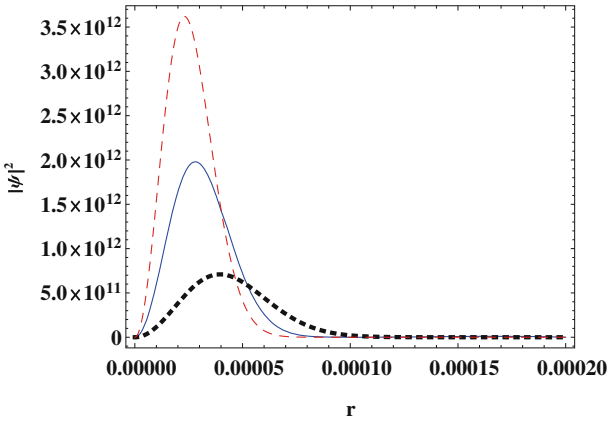

Figure 12. Density profile for the BEC in generalized Pöschl–Teller potential corresponding to the change in n_{exc}. The thick dotted black line is for $n_{\text{exc}} = 50$, the blue solid line is for $n_{\text{exc}} = 100$ and the red dashed line is for $n_{\text{exc}} = 150$. Here $\eta = 1$ and $\beta = 1$.

For noninteracting BEC, the ground-state solution is the ground-state solution of the Schrödinger equation itself. Thus, the density profile for the ground state is important. We present the density profile for the ground state with respect to the choices of the number of excited states n_{exc}, corresponding to the change in η, as these two parameters determine the strength of the confining potential and also corresponding to different choices of parameter β, which decides the shape of the potential. Absolute square of the normalized wave function gives the density profile. Here we normalized the wave function numerically between $r = 0$ and $r = 2 \times 10^{-4}$. The density profiles are shown in figures 12–14, for the three cases discussed above.

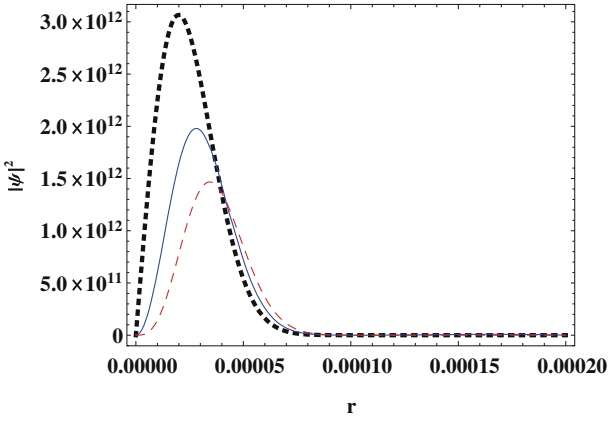

Figure 13. Density profile for the BEC in generalized Pöschl–Teller potential corresponding to the change in β. The thick dotted black line is for $\beta = 0.5$, the blue solid line is for $\beta = 1$ and the red dashed line is for $\beta = 1.5$. Here $\eta = 1$ and $n_{\text{exc}} = 100$.

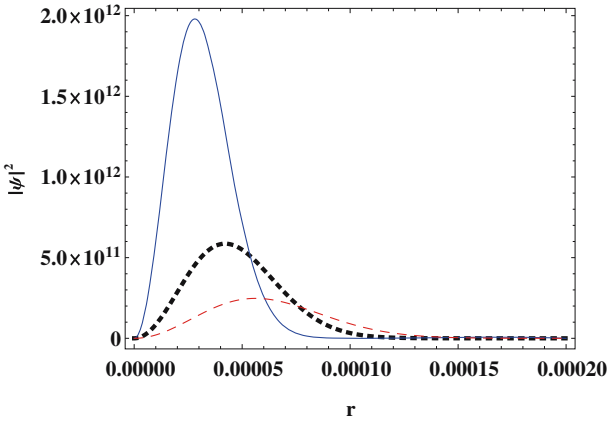

Figure 14. Density profile for the BEC in generalized Pöschl–Teller potential corresponding to the change in η. The blue solid line is for $\eta = 1$, the thick dotted black line is for $\eta = 1.5$ and the red dashed line is for $\eta = 2$. Here $\beta = 1$ and $n_{\text{exc}} = 100$.

Figures 12 and 14 show the results as we expected. As the confined gas becomes free, the density profiles spread over the limit. However, density profile shown in figure 14 indicates that, even though the dynamics does not depend on β tuning, the ground-state solution depends on it. Thus, by suitable tuning of β, the phase-space density can be modified without affecting the dynamics and can enhance the quality of the condensate.

4. Conclusion

We have analysed and modified the generalized Pöschl–Teller potential given in unknown parameters A, B and α to the potential form with parameters which are physically meaningful. This modification of the generalized Pöschl–Teller potential and the particular choice of the parameters allow us a means to control the number of excited states, shape of the potential and also the strength of the confinement. We can tune the generalized Pöschl–Teller potential from a strong confining potential to a free particle one by suitably tuning n_{exc} and η, whereas the shape of the generalized Pöschl–Teller potential can be tuned from a funnel shape to a Morse potential shape by the suitable tuning of β. Furthermore, we have obtained the energy eigenvalue for the actual generalized Pöschl–Teller potential from the SUSY QM solution.

The dynamics of noninteracting BEC of ^{39}K atoms trapped in the generalized Pöschl–Teller potential have been studied with respect to the n_{exc} and η tunings. The effect of such tuning on the condensate fraction (N_0/N) as well as on the chemical potential is an important result which may find applications in quantum information technology and quantum computers. As the solution of the Schrödinger equation for the potential does not depend on β, the dynamics have no dependence on it. However, the density profile for the ground-state solution of the noninteracting BEC depends on n_{exc}, β and η parameters. The β tuning can be used to enhance the quality of the condensate, without affecting the dynamics of the condensate.

Acknowledgements

One of the authors, SR acknowledges the support and facility extended to him by the Hadron Physics Group, Department of Physics, Sardar Patel University. He also expresses sincere thanks to Dr Bobby K Antony, Department of Applied Physics, Indian School of Mines, Dhanbad for his support and guidance.

References

[1] A Einstein, *Sitzungsber. Preuss. Akad. Wiss., Phys. Math. Kl.* 261 (1924); 3 (1925)
[2] S N Bose, *Z. Phys.* **26**, 78 (1924)
[3] F London, *Phys. Rev.* **54**, 947 (1938)
[4] K B Davis *et al*, *Phys. Rev. Lett.* **75**, 3969 (1995)
[5] M H Anderson, J R Ensher, M R Matthews, C E Wieman and E A Cornell, *Science* **269**, 198 (1995)
[6] C C Bradley, C A Sackett, J J Tollett and R G Hulet, *Phys. Rev. Lett.* **75**, 1687 (1995)
[7] arXiv:cond-mat/0502539 [cond-mat.other]
[8] P W H Pinkse, A Mosk, M Weidemüller, M W Reynolds, T W Hijmans and J T M Walraven, *Phys. Rev. Lett.* **78**, 990 (1997)
[9] F Cooper, A Khare and U Sukhature, *Phys. Rep.* **251**, 267 (1990)
[10] arXiv:1309.1448v3 [quant-ph]
[11] K Burnett, P S Julienne, P D Lett, E Tiesinga and C J Williams, *Nature (London)* **416**, 225 (2002)
[12] arXiv:cond-mat/0703714v1 [cond-mat.other], 27 March 2007
[13] P W Anderson, *Phys. Rev.* **109**, 1492 (1958)
[14] See for example J E Lye, L Fallani, C Fort, V Guarrera, M Modugno, D S Wiersma and M Inguscio, arXiv:cond-mat/0611146v1 [cond-mat.other], 6 November 2006, and references therein
[15] B P Anderson and M A Kasevich, *Science* **282**, 1686 (1998)
[16] Y Shin, M Saba, T A Pasquini, W Ketterle, D E Pritchard and A E Leanhardt, *Phys. Rev. Lett.* **92**, 050405 (2004)
[17] G Roati, E de Mirandes, F Ferlaino, H Ott, G Modugno and M Inguscio, *Phys. Rev. Lett.* **92**, 230402 (2004)
[18] H Uncu, D Tarhan, E Demiralp and O E Müstecaplioğlu, *Phys. Rev. A* **76**, 013618 (2007)